Nucleic Acids Research Advance Access published August 24, 2010

Nucleic Acids Research, 2010, 1–12
doi:10.1093/nar/gkq723

The phosphate clamp: a small and independent motif for nucleic acid backbone recognition

Seiji Komeda[1,2,4], Tinoush Moulaei[1], Masahiko Chikuma[2], Akira Odani[3], Ralph Kipping[4], Nicholas P. Farrell[4,*] and Loren Dean Williams[1,*]

[1]School of Chemistry and Biochemistry, Georgia Institute of Technology, Atlanta, GA 30332-0400, USA, [2]Osaka University of Pharmaceutical Sciences, Takatsuki, 569-1094, [3]Institute of Medical, Pharmaceutical and Health Sciences, Kanazawa University, Kakuma-machi, Kanazawa, 920-1192, Japan and [4]Department of Chemistry, Virginia Commonwealth University, Richmond, VA 23284-2006, USA

Received April 18, 2010; Revised July 13, 2010; Accepted July 31, 2010

ABSTRACT

The 1.7 Å X-ray crystal structure of the B-DNA dodecamer, $[d(CGCGAATTCGCG)]_2$ (DDD)-bound non-covalently to a platinum(II) complex, $[\{Pt(NH_3)_3\}_2$-μ-{*trans*-$Pt(NH_3)_2(NH_2(CH_2)_6NH_2)_2\}](NO_3)_6$ (1, TriplatinNC-A,) shows the trinuclear cation extended along the phosphate backbone and bridging the minor groove. The square planar tetra-am(m)ine Pt(II) units form bidentate N-O-N complexes with OP atoms, in a Phosphate Clamp motif. The geometry is conserved and the interaction prefers O2P over O1P atoms (frequency of interaction is O2P > O1P, base and sugar oxygens > N). The binding mode is very similar to that reported for the DDD and $[\{$*trans*-$Pt(NH_3)_2(NH_2(CH_2)_6(NH_3^+)\}_2$-μ-{*trans*-$Pt(NH_3)_2(NH_2(CH_2)_6NH_2)_2\}](NO_3)_8$ (3, Triplatin NC), which exhibits *in vivo* anti-tumour activity. In the present case, only three sets of Phosphate Clamps were found because one of the three Pt(II) coordination spheres was not clearly observed and was characterized as a bare Pt^{2+} ion. Based on the electron density, the relative occupancy of DDD and the sum of three Pt(II) atoms in the DDD-1 complex was 1:1.69, whereas the ratio for DDD-2 was 1:2.85, almost the mixing ratio in the crystallization drop. The high repetition and geometric regularity of the motif suggests that it can be developed as a modular nucleic acid binding device with general utility.

INTRODUCTION

Since the discovery of its' anti-tumour activity the mononuclear platinum drug *cis*-platin {*cis*-$[PtCl_2(NH_3)_2]$, *cis*-diamminedichloridoplatinum(II)}, (1,2), and subsequently the related carboplatin {$[Pt(NH_3)_2$(CBDCA)], *cis*-diammine [1,1-cyclobutandicarboxylato) platinum(II)} and oxaliplatin {[Pt(R,R-dach)(ox)], 1,2-*R*, *R*-diaminocyclohexane(oxalato)platinum(II)} have contributed significantly to the anti-cancer drug armamentarium. The drugs all form predominantly short-range 1,2-intrastrand crosslinks on DNA which cause severe conformational distortion, the specific nature of which is thought to be a critical determinant of the biological consequences of platinum drug treatment (3–6). Polynuclear Pt(II) agents are structurally and biologically distinct from mononuclear Pt(II) agents, and form long-range (Pt,Pt) inter- and intra-strand crosslinks (7–14). The DNA conformational distortions induced by polynuclear agents are thus structurally distinct from those of *cis*-$[PtX_2(amine)_2]$, and are not necessarily susceptible to the same cellular processing as cisplatin and other *cis*-$[PtX_2(amine)_2]$ chemotypes (14). The development of cellular resistance to cisplatin (15,16) and also to carboplatin and oxaliplatin (17), through enhanced DNA repair, might thus be circumvented in polynuclear agents. The advancement to Phase II human clinical trials of the prototypical trinuclear drug BBR3464 (for all structures, see Figure 1) validates the search for structure diversity in new platinum analogues (13,18).

Replacement of the substitution-labile chlorides of BBR3464 by ammonia (ammine) or amines gives the non-reactive polynuclear agents TriplatinNC-A (**1**, Figure 1A) and TriplatinNC (**2**, Figure 1B). Crystallographic characterization of a DNA complex with **2** (19) shows that the two mutually *cis*-oriented platinum-a(m)mine groups of the PtN_4 units form discrete NH•••OP•••HN (amine•••phosphate•••ammine)-binding motifs. These 'Phosphate Clamps' represent a discrete new ligand–DNA-binding mode, extending the repertoire of binding possibilities by

*To whom correspondence should be addressed. Tel: +1 804 828 6320; Fax: +1 804 828 8599; Email: npfarrell@vcu.edu
Correspondence may also be addressed to Loren Dean Williams. Tel: +1 404 894 9752; Fax: +1 404 894 7452; Email: williams@chemistry.gatech.edu

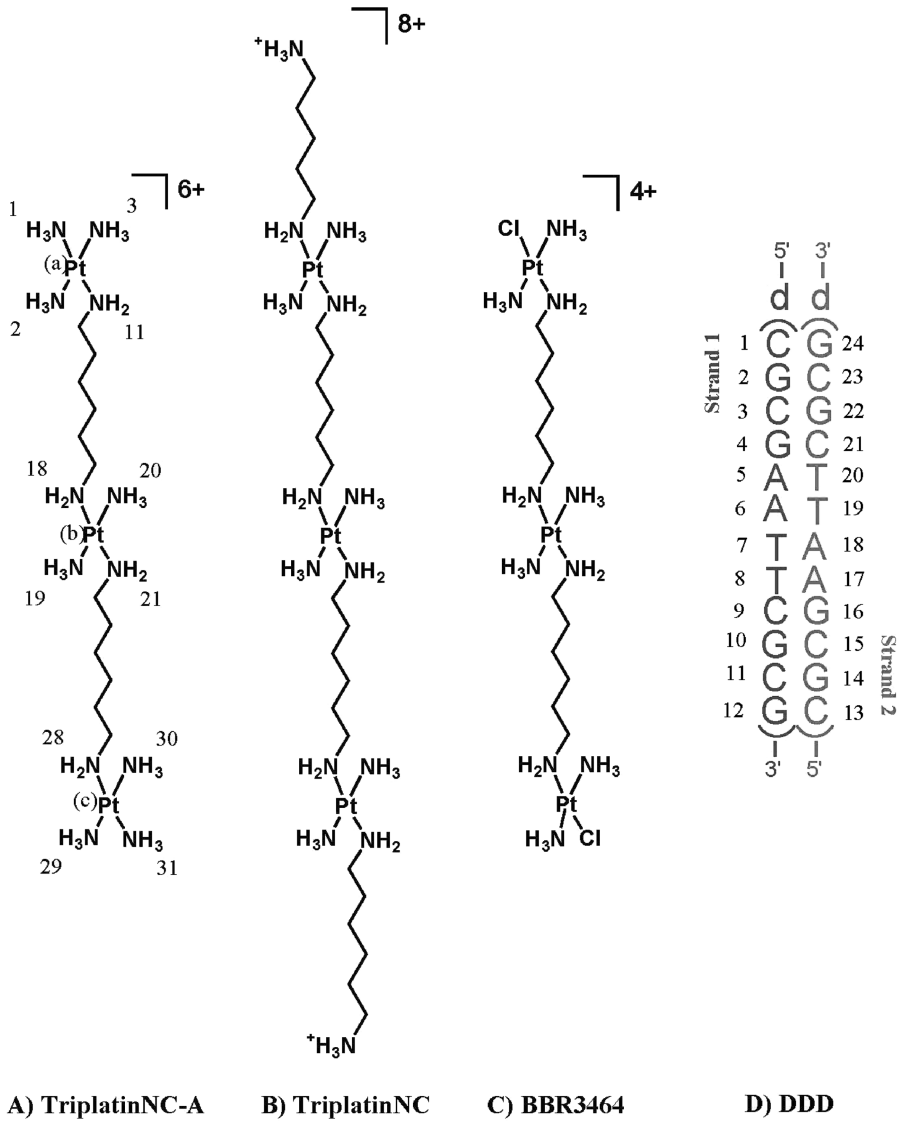

Figure 1. The chemical structures of the trinuclear platinum(II) compounds discussed in this article: (**A**) TriplatinNC-A, ([{$Pt(NH_3)_3$}$_2$-μ-{*trans*-$Pt(NH_3)_2(NH_2(CH_2)_6NH_2)_2$}]$(NO_3)_6$, **1**, 0,0,0/t,t,t,). (**B**) Triplatin-NC, ([{*trans*-$Pt(NH_3)_2(NH_2(CH_2)_6(NH_3^+)$}$_2$-$\mu$-{*trans*-$Pt(NH_3)_2$ (NH_2 $(CH_2)_6$ $NH_2)_2$}]$(NO_3)_8$, **2**). (**C**) BBR3464 containing substitution-labile chlorides ([{*trans*-$PtCl(NH_3)_2$}$_2$-μ-{*trans*-$Pt(NH_3)_2(NH_2(CH_2)_6NH_2)_2$}]$(NO_3)_4$, **3**). (**D**) The double-stranded self-complementary dodecamer duplex, [d(CGCGAATTCGCG)]$_2$ (DDD), used for this crystallographic study.

small ligands beyond intercalation and groove binding. Non-covalent polynuclear platinum compounds and TriplatinNC in particular, have interesting biological properties including *in vitro* cytotoxicity, anti-tumour activity and high cellular accumulation (20–23).

The quasi-independent and modular nature of the PtN_4-based phosphate clamp as observed in the TriplatinNC–DNA complex suggests that the interaction can be used as a general DNA-binding element in combination with other nucleic acid binding motifs. The mode of association (B-form backbone tracking, A-form backbone tracking, groove spanning, intra-molecular association, etc.) can be dictated by alteration of linker chain length and rigidity, charge distribution and the number of PtN_4 units. To examine the utility and generality of the phosphate clamp we have extended the study of non-covalent platinum complexes to TriplatinNC-A (Figure 1A). This compound is differentiated from TriplatinNC by the absence of dangling amines on the terminal Pt(II) atoms, resulting in a more compact molecule and an overall charge of 6+ instead of 8+. Here we describe the 3D X-ray crystal structure of **1** bound to the Dickerson–Drew Dodecamer (DDD, Figure 1D) (24), the self-complementary double-stranded DNA [d(CGCGAATT CGCG)]$_2$. The binding modes and consequent conformational distortions of both platinum complexes are compared and the biological relevance discussed.

EXPERIMENTAL PROCEDURES

Synthesis

TriplatinNC-A, a gift of Alex Hegmans, was prepared by published procedures (20).

Crystallization

The ammonium salt of reverse-phase HPLC-purified d(CGCGAATTCGCG) (DDD, Integrated DNA Technologies, Coralville, IA, USA) was combined with TriplatinNC-A. The crystallization conditions were the same as for DDD–TriplatinNC complex (19). Crystals were grown in hanging drops by vapor diffusion from a solution initially containing 0.19 mM of the duplex, [d(CGCGAATTCGCG)]$_2$, 0.19 mM TriplatinNC-A, 31 mM sodium cacodylate, pH 6.5, 9.6 mM magnesium chloride and 6.9% 2-methyl-2,4-pentanediol (MPD). The crystallization solution was equilibrated against a reservoir of 30% MPD at 20°C in a constant-temperature incubator. Orthorhombic ($P2_12_12_1$) crystals appeared within a month. The crystal chosen for data collection was $0.1 \times 0.1 \times 0.2$ mm^3.

Data collection

Diffraction data were collected on beamline X26C at the National Synchrotron Light Source, Brookhaven National Laboratory. A total of 120 frames of intensity data (oscillation angle = 1.0°) were collected at 175 K at a wavelength of 1.05 Å and recorded on an ADSC-Quantum 4 CCD detector. Data were merged and reduced with HKL2000 (25).

Structure solution and refinement

The starting DNA model consisted of coordinates of [d(CGCGAATTCGCG)]$_2$ (24), [NDB entry bdl084 (25)] excluding solvent and ions. After a rotation/translation search and rigid body refinement with CNS version 1.1 (26), the R/R-free factor were 52/55. Strong sum and difference peaks indicated positions of three Pt^{2+} atoms, which were added to the model, giving R/R-free factor of 38/39. The R/R-free factor dropped to 20/26 upon addition of 83 water molecules along with additional atoms of TriplatinNC-A. A partially occupied/disordered TriplatinNC-A was modeled as a bare Pt^{2+} ion. The initial model of TriplatinNC-A was generated with Chem3D Pro version 4.0 (CambridgeSoft).

The three Pt^{2+} positions were confirmed by anomalous maps, which were computed using phases of only a single Pt^{2+} atom, with the program CNS. During the refinement a peak of electron density surrounded by four water molecules, forming a partially disordered octahedron, was assigned as a sodium ion. The four Na^+–O bond lengths are 2.03, 2.30, 2.43 and 2.52 Å, respectively for Na^+–O1, Na^+–O2, Na^+–O3, and Na^+–O4. The bond length of Na^+–O1 is significantly shorter than the others and rather close to that for a Mg^{2+}–O bond. However, replacement of Mg^{2+} for Na^+ resulted in an increase in R/R-free factor by 0.21/0.03%. The occupancies of TriplatinNC-A were estimated using the Pt^{2+} atoms. Occupancies were optimized throughout the refinement by fitting statistics and by examination of $\pm(F_o–F_c)$ maps. Thirty-five cycles of refinement were carried out using the program CNS version 1.1 (27), during which isotropic thermal factor refinement was performed for all the atoms. The refinement converged to a final R/R-free factor of 19.59/25.80. Helical parameters were calculated using a program CURVES 5.3 (28).

Circular dichroism spectroscopy

Circular dichroism (CD) spectra were recorded at room temperature using a Jasco 600 CD spectrophotometer and a 10 mm quartz submicro cuvette. All samples were prepared in 10 mM phosphate buffer solution, pH 7.4 containing 50 mM sodium chloride. The dodecamer (100 μM in nucleotides) was incubated with the corresponding platinum compounds at 37°C for 1 h at variable r_i values [r_i = (initial number of molecules of platinum complex in solution)/(number of nucleotides of DNA in solution)]. To obtain the presented spectra six scans in the range from 200 to 350 nm were averaged. The background was subtracted electronically.

RESULTS

Diffraction data from crystals of the complex formed between the DDD and **1** extend to 1.70 Å. Data collection and refinement statistics are given in Table 1. The maps surrounding the DNA are clean and generally continuous (Figure 2A). The final refined model of the asymmetric unit contains (i) one DNA duplex with 12 bp, (ii) a partially ordered and partially occupied molecule of TriplatinNC-A, with two Pt coordination spheres, one hexanediamine bridge with all six carbon atoms and a total of eight nitrogen atoms from the two coordination spheres, (iii) a tetra-hydrated Na^+ ion and (iv) 87 water molecules including the first shell Na^+ water molecules. One Pt^{2+} ion lacking ligands is also observed. The occupancy of the ordered portion of **1**, with two Pt^{2+} ions plus their coordination spheres linked by the hexanediamine bridge, is estimated to be 79%. The occupancy of the bare Pt^{+2} ion is estimated to be 11%.

Platinum positions were initially established from the intense peaks in the sum ($2F_o - F_c$) maps, and were confirmed by the anomalous peaks ($F_+ - F_-$, Figure 2B). The anomalous electron density is consistent with the Pt^{2+} positions initially determined with the sum electron density map.

Phosphate clamps

The Pt-am(m)ine groups of **1** (TriplatinNC-A) form a total of 12 hydrogen bonds with DNA (Figure 3). The compound, like **2** (TriplatinNC), shows remarkable selectivity for (i) DNA oxygen atoms over nitrogen atoms, (ii) phosphate oxygen atoms over other oxygen atoms and (iii) for O2P over O1P atoms. As a result, 11 of the hydrogen bonding interactions involve oxygen atoms, 10 of which are with phosphate oxygens. The exception is a hydrogen bond to a guanine O6. Only a single hydrogen bond links an NH_3 group of a PtN_4 unit to a nitrogen atom (N7 of G).

The hydrogen-bonding interaction between the ligand (Pt complex) and DNA is best structurally characterized by the formation of phosphate clamps (Figure 3). In the phosphate clamp, a single OP atom accepts two hydrogen bonds, one from each of two adjacent a(m)mino groups of

Table 1. Data collection and refinement statistics

Unit cell dimensions	$\alpha = \beta = \gamma = 90°$ $a = 23.440$ Å, $b = 39.007$ Å $c = 65.922$ Å
DNA (asymmetric unit)	$[d(CGCGAATTCGCG)]_2$
Space group	$P2_12_12_1$
Temperature of data collection (K)	175
Number of all reflections	10 298
Number of reflections in resolution range (1.7–25 Å)	6843
Number of reflections used in refinement ($F > 3\sigma F$)	6292
RMSD of bonds from ideality (Å)	0.026
RMSD of angles from ideality (°)	1.995
Max. resolution of observed reflections (Å)	1.26
Max. resolution of refinement (Å)	1.70
Number of DNA atoms	486
Number of TriplatinNC-A atoms	15
Number of water molecules, excluding sodium first shell	83
Number of sodium ions plus coordinating water molecules	5
R-factor (%, $F > 3\sigma F$)	19.64
R-free (%, all)	25.68

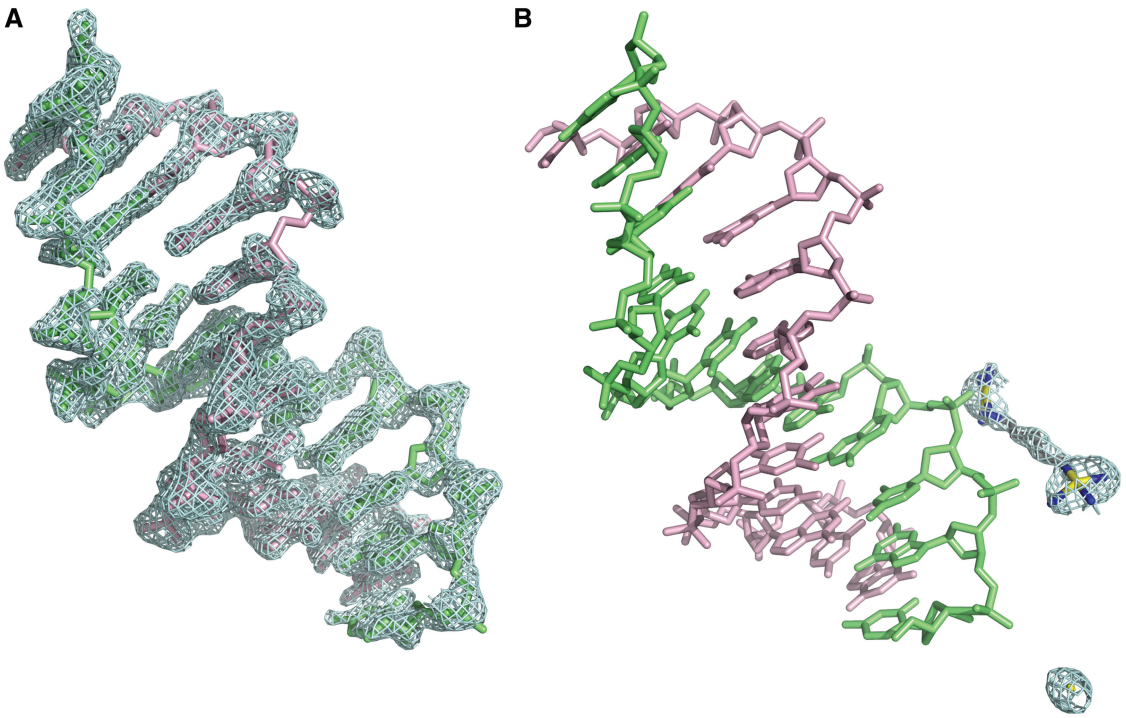

Figure 2. Electron density maps surrounding the DDD/**1** (TriplatinNC-A) complex. (**A**) Sum ($2F_o$–F_c) electron density surrounding the DNA, contoured at 1.3σ. (**B**) Sum electron density around **1** contoured at 1.0σ.

a PtN_4 unit. Three phosphate clamps involving two PtN_4 coordination spheres of TriplatinNC-A are evident in the electron density. In the case of **2**, seven phosphate clamps involving four Pt^{2+} centers were observed (19). Similar to the previous structure, **1** forms an extensive hydrogen bonding and electrostatic network within the DDD crystal, bridging a total of five different symmetry-related duplexes (Figure 3).

In the structure discussed here and the previous one (19), the geometries of Phosphate Clamps are highly conserved. The motif again appears to require *cis*-orientation of the am(m)ine ligands—mutually *trans* ligands do not participate in phosphate clamps. Furthermore, the ligands are one Pt-NH_3 (ammine) group and one Pt-NH_2R group. Only two PtN_4 units are observable, which collectively engage in three phosphate clamps. In this structure, one Pt atom, designated Pt(a), was assigned as a bare cation since the electron density around Pt(a) is not sufficient to determine the geometry of the coordination sphere.

Backbone tracking

The observable portion of TriplatinNC-A is extended along the backbone of one strand of the DDD (Sym 0 in Figure 3). One Phosphate Clamp [Pt(b)] engages the

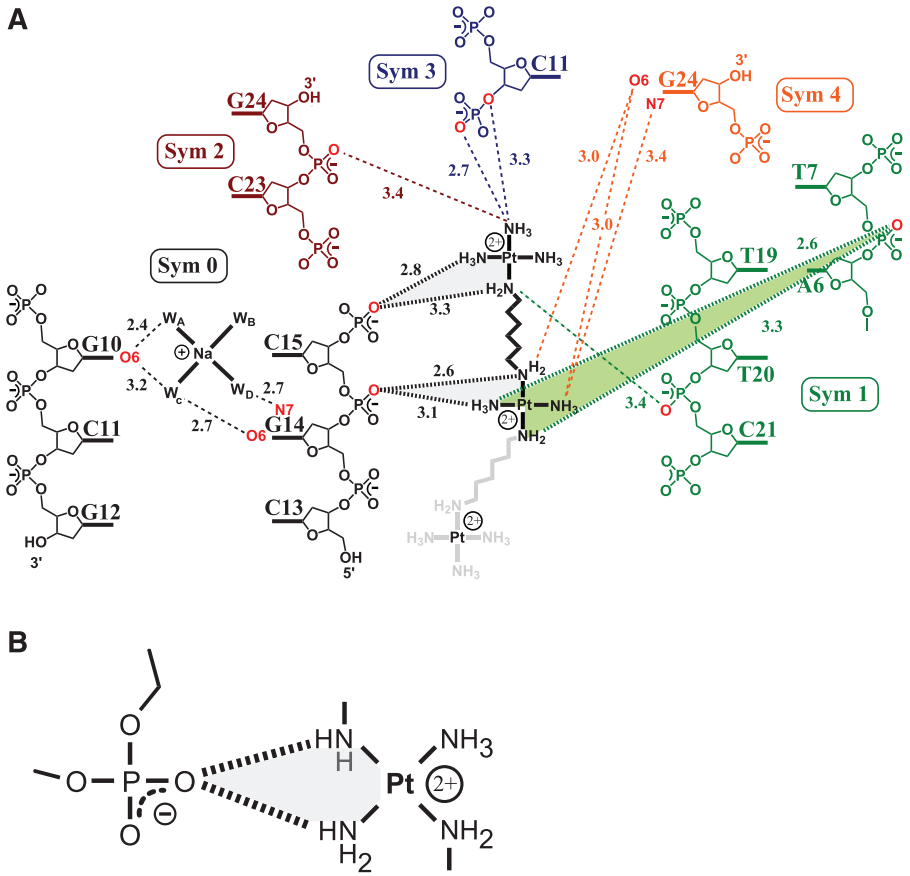

Figure 3. Hydrogen bonding interactions of **1** with DNA. Hydrogen bonding interactions of phosphate clamps are indicated by bold hashed lines. The phosphate clamps are highlighted by shading. Other hydrogen bonds are indicated by dashed lines. (**A**) **1** forms three phosphate clamps with the DNA. Oxygen and nitrogen atoms that form hydrogen bonds with **1** or the Na^+ are highlighted in red. Hydrogen bonding distances are given in Ångstroms. The symmetry operators are as follows : Sym 0: x,y,z; Sym 1: –x,y–1/2,–z+3/2; Sym 2: –x–1/2,–y+1,z–1/2; Sym 3: x–1,y,z; Sym 4: –x + 1/2,–y+1,z–1/2. (**B**) A schematic diagram of a phosphate clamp.

O2P oxygen atom of C15 while the other [Pt(c)] engages the O2P atom of the adjacent G16 (Figure 4). In contrast, in the DDD–TriplatinNC complex the PtN_4 units forms phosphate clamps with A17 and G16, but not with C15 (19). This difference in binding interactions may be due to the increased charge caused by the presence of the dangling hexanediamine, which forms hydrogen bonds with the O2P of G14 (19). This extra interaction appears to induce the trinuclear unit to bend, pushing the one PtN_4 coordination sphere away from the phosphate of C15, forming a total of three phosphate clamps.

Groove spanning

TriplatinNC-A participates in Groove Spanning by bridging between two DNA strands across the minor groove of the DNA duplex (Duplex Sym 1 in Figure 3) through clamps at the phosphate of T7 and one incomplete clamp, a PtN_4-O2P hydrogen bond at C21 (Figures 3 and 5). In contrast, in the TriplatinNC–DDD complex the Groove Spanning is achieved by two intact phosphate clamps. Overall, the two compounds bind by remarkably similar motifs—the Backbone Tracking and Groove Spanning are facilitated through the Phosphate Clamp, although the specific positions and interacting parts of the DDD are not exactly the same.

Sodium ions

In many previously-described high-resolution DDD crystal structures, a fully hydrated magnesium ion $[Mg(H_2O)_6]^{2+}$ is located in the major-groove near one end of the duplex (25,29,30). The first shell water molecules of the Mg^{2+} ion form hydrogen bonds to the G(2)–C(23) and C(3)–G(22) base pairs. In the DDD-**1** complex, a hydrated sodium ion $[Na(H_2O)_4]^+$ is observed on the other end of the duplex in the major groove adjacent to G(10)–C(15) and C(11)–G(14). The Na^+ does not form first-shell contacts with the DNA. Instead, the four first-shell water molecules that coordinate the Na^+ form hydrogen bonds to the guanine O6 and N7 positions of G(14) and to the O6 position of G(10), Figure 3. These hydrogen bonds are similar to those of $[Mg(H_2O)_6]^{2+}$ at the other end of the DNA fragment. This Na^+ ion is nearby to where **1** tracks the DNA backbone. In the DDD-**2** complex a hexa-coordinate sodium ion $[Na(H_2O)_5(O6)]^+$ is also observed, with the sixth ligand being the O6 from residue G(22). The first shell water ligands interact with G(2), C(21) and G(22)

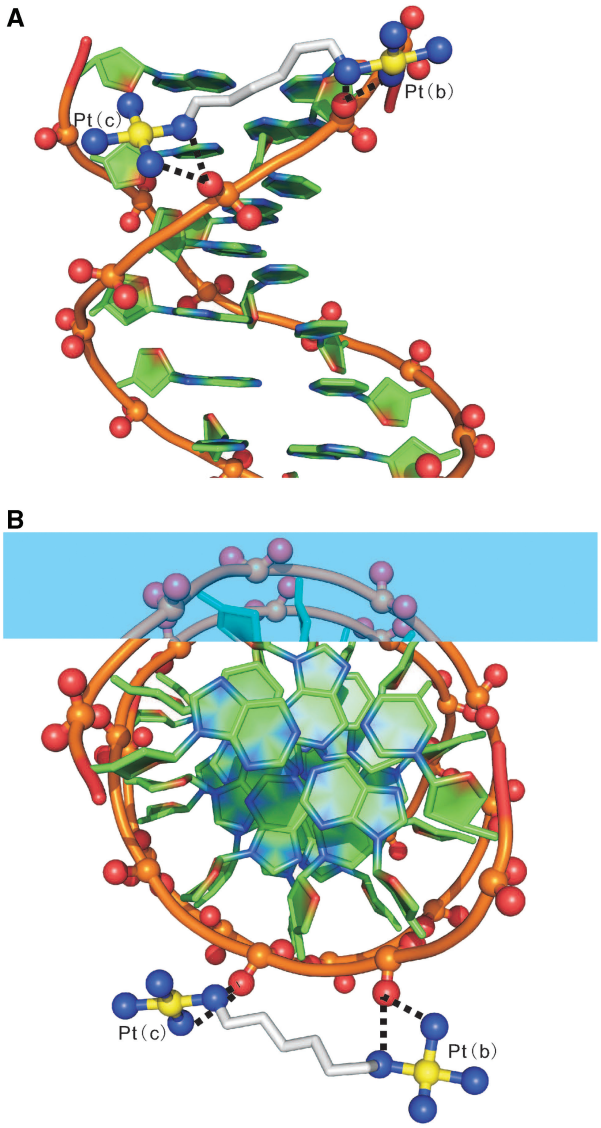

Figure 4. Backbone tracking of the phosphate clamp. Hydrogen bonds between **1** and DNA are indicated by dashed lines. Two phosphate clamps are illustrated. (**A**) View perpendicular to the helical axis. (**B**) View along the helical axis. Atoms are colored by type with carbon (DNA), green; carbon (TriplatinNC-A) grey; nitrogen, blue; oxygen, red; platinum, yellow. The phosphodiester backbone of the DNA is represented by a tube. The P, O1P and O2P atoms are ball-and-stick. TriplatinNC-A is represented by stick, except for nitrogen and platinum atoms, which are ball-and-stick. This and some of the other figures in this manuscript were made in part with Pymol (Warren L. DeLano 'The PyMOL Molecular Graphic System.' DeLano Scientific LLC, San Carlos, CA, USA http://www.pymol.org).

and the complex is located at the opposite end of DDD from where **2** forms the Backbone Tracking (19). Accordingly, the location and hydrogen bonding properties of hydrated sodium cations, although observed in both cases, were different between the two structures.

DNA conformation

To examine the DNA conformational changes induced through binding by this class of ligand, we compare the DDD–TriplatinNC-A (**1**) to DDD–TriplatinNC (**2**) and to other high resolution DDD structures, in particular structure bdl084, which is the highest resolution, non-modified DDD structure determined thus far (25). Phosphodiester backbone torsion angles, glycosyl angles and sugar puckers are given in Table 2. The major-groove and minor-groove widths of DDD–TriplatinNC-A are intermediate between those of DDD–TriplatinNC and the control DDD, Figure 6. From these parameters, the superimposition of both polynuclear complexes onto the control DDD is shown in Figure 7. Base–base and inter-base parameters are shown in Supplementary Figures S1 and S2.

Previously we suggested that an observed increase in the minor groove width of DDD–TriplatinNC in comparison to the 'free' DDD is related to the groove spanning by the complex. The cationic centers of **1** interact with the same phosphates as TriplatinNC. In both structures, two Phosphate Clamps are juxtaposed across the minor groove. However, in the present case, one of the two Phosphate Clamps of the Groove Spanning mode is only partially formed (see above). The weaker Groove Spanning interactions might result in slightly lesser deformation of the duplex. For example, the major-groove width of DDD-**1** at A(6)–T(19), in which the major-groove width of DDD–TriplatinNC and the control DDD show the largest deviation, was found to be the median value of the other two structures, Figure 6.

The backbone: BI versus BII. The DNA complexed with TriplatinNC-A is wholly in the BI conformation, with ε–ξ is in the range of −160 to +20. B-DNA conformation is characterized by BI, the most frequent, or BII, depending on the torsion angles ε and ξ (31,32). These torsion angles influence the positions of phosphate groups and modulate the width of the minor groove. The difference between ε and ξ is a useful indicator of BI/BII. An ε–ξ of roughly −90° indicates BI whereas a value of roughly +90° indicates BII.

The backbone: sugar puckers. Of the 24 sugar puckers of DDD-**1,** 11 differ from those of the corresponding residues in the control DDD. A total of 14 differ from those of DDD–TriplatinNC. Large differences in sugar pucker are found in G(12) (−103) and (C23) (+99) compared to the control DDD. Differences are also found in G(2) (+168), C(3) (+93) C23 (+99) relative to DDD–TriplatinNC.

Global conformation. The axial bending and axial shortening of the DDD-**1** complex are very similar to those of DDD–TriplatinNC and significantly greater than those of the DDD. In the program Curves 5.3 (28), UU is a measure of axial bending, giving the angle formed by the axis segments of the terminal sections of the DNA duplex. PP is the angle between the vectors formed between the two axis reference points at either end of the fragment. UU and PP for the DDD-**1** complex were found to be 28° and 38°, both of which are very close to the

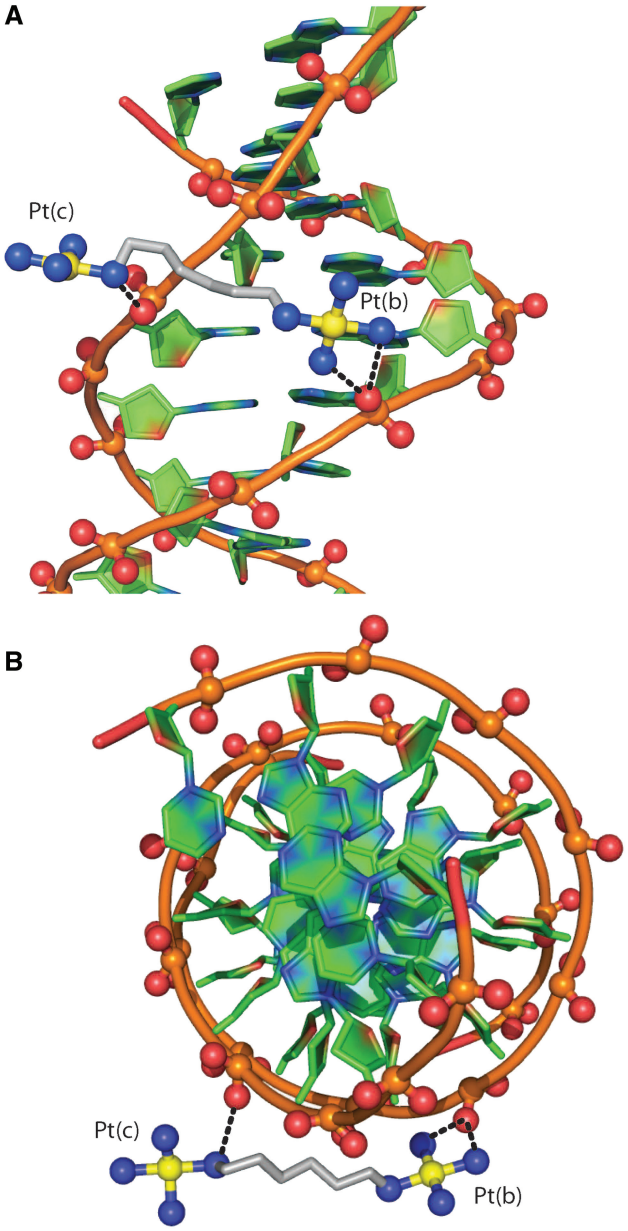

Figure 5. Groove spanning. Hydrogen bonds between **1** and DNA (Sym 1, Figure 3) are indicated by dashed lines. There are two Phosphate Clamps, with which TriplatinNC-A bridges two strands across the minor groove of a DNA duplex, at the lip of the minor groove, defined in Sines *et al.* (29). (**A**) View perpendicular to the helical axis. (**B**) View along the helical axis. Atoms are colored and coded as in Figure 4.

corresponding value of the DDD–TriplatinNC complex and significantly larger than those of the control DDD. This trend is also the same in axial bend and the axial path length shortening ratio (DDD-**1**: 28°/2.0%; DDD–TriplatinNC: 27°/2.4%; DDD: 12.9°/0.66%).

Conformation in solution

The similarity in binding mode of the two polynuclear complexes is also confirmed in solution. The CD spectra of the DDD titrated with both **1** and **2** are very similar and further confirm the essential B-nature of the conformational changes upon complex binding (Figure 8). The spectra are characterized by a negative shift (decrease) in ellipticity for the peak centered at 280 nm and a concomitant positive shift (increase) for the peak centered at 206 nm. Thus the difference in peak height is decreased.

DISCUSSION

The results reported here confirm the generality and utility of the PtN_4 unit for formation of Phosphate Clamps with DNA, involving two modes of binding, Backbone Tracking and Groove Spanning. Phosphate clamps form six-membered rings, with two hydrogen bonds from *cis*-oriented Pt-a(m)mines to a common phosphate oxygen. It is a discrete and modular DNA-binding device with high potential as a drug-design scaffold. In solution, conformational changes are equivalent for the two complexes whose structures have been determined, further emphasizing the similarity in binding mode.

Forks and clamps

The interactions of PtN_4 coordination units with DNA have some analogy to the interactions of the guanidino group of arginine with polynucleotides. The limiting 'canonical' structures for both arginine forks and phosphate clamps are shown schematically below for comparison. It was previously suggested that arginine shows an OP clamping ability in which two adjacent NH groups of a guanidino group interact with two oxygen atoms of a common phosphate (33–35). This motif would result in an eight-membered ring (including hydrogen atoms) stabilized by two hydrogen bonds. In the 'Arginine Fork', one guanidino group may be engaged in two of these interactions (33). The apparent mimicry of arginine by the platinum–tetra(m)mine unit led us re-evaluate the frequency and geometry of Arginine Forks. We therefore examined ribosomal structures such as 1JJ2 (35) and 2J00/2J01 (34). The large subunit of the *Haloarcula Marismortui* ribosome (1JJ2), for example, contains 336 arginines and nearly 3000 phosphate groups. From analysis of such structures we conclude that the guanidino group of arginine, like PtN_4, binds to nucleic acids with high selectivity for OP atoms, i.e. for non-bridging phosphate oxygens, but with phosphate oxygen selectivity: $PtN_4 > ARG$. The guanidino group does form clamp-like structures, consisting of eight-membered rings, at some measurable frequency but again, $PtN_4 >> ARG$. However PtN_4 forms forks while the guanidino group of arginine does not; the frequency at which one guanidino group engages in two phosphate clamps is essentially zero. In sum, PtN_4 appears to be unique in its combined selectivity for OP atoms, forking propensity, and highly conserved geometry of binding. Thus the PtN_4 unit has

Table 2. Backbone torsion angles (α–ζ), glycosyl angles (χ), pseudorotation phase angles and amplitudes, and sugar puckers[a]

Residue	χ (°)	γ (°)	δ (°)	ε (°)	ζ (°)	α (°)	β (°)	Phase (°)	Amplitude	Pucker
C(1)	–121	71	128	–179	–124	–38	–177	133	40	C1′-exo
G(2)	–113	35	146	–173	–104	–58	167	170	32	C2′-endo
C(3)	–129	55	112	–164	–105	–49	176	111	34	C1′-exo
G(4)	–94	45	139	174	–101	–38	–177	168	32	C2′-endo
A(5)	–100	33	138	179	–105	–53	174	169	31	C2′-endo
A(6)	–113	50	129	–178	–91	–64	175	155	30	C2′-endo
T(7)	–125	53	110	178	–102	–53	166	108	39	O1′-endo
T(8)	–116	61	129	–178	–105	–47	177	141	34	C1′-exo
C(9)	–107	46	134	–165	–92	–68	167	154	33	C2′-endo
G(10	–91	49	144	–109	160	–74	154	146	45	C2′-endo
C(11)	–106	48	137	–163	–88	–61	170	157	30	C2′-endo
G(12)	–104	45	101					104	37	O1′-endo
G(24)	–143	44	87					48	34	C4′-exo
C(23)	–125	52	117	–171	–95	–57	168	116	31	C1′-exo
G(22)	–82	40	152	–128	–175	–76	144	150	49	C2′-endo
C(21)	–109	42	123	–169	–88	–59	173	129	35	C1′-exo
T(20)	–123	57	121	–175	–97	–56	177	123	34	C1′-exo
T(19)	–127	59	115	–179	–91	–62	175	117	36	C1′-exo
A(18)	–120	50	113	170	–89	–59	173	111	37	C1′-exo
A(17)	–103	51	155	–173	–108	–60	169	181	38	C3′-exo
G(16)	–104	61	145	163	–98	–55	–166	169	33	C2′-endo
C(15)	–133	54	100	–176	–89	–65	179	70	30	C4′-exo
G(14)	–109	–142	142	–174	–97	–53	160	169	27	C2′-endo
C(13)	–175	172	155	–108	–77	73	–152	207	35	C3′-exo

[a]Backbone torsion angles are O3′-P-α-O5′-β-C5′-γ-C4′-δ-C3′-ε-O3′-ζ-P-O5′.

potential as a general DNA/RNA-binding element and drug design scaffold.

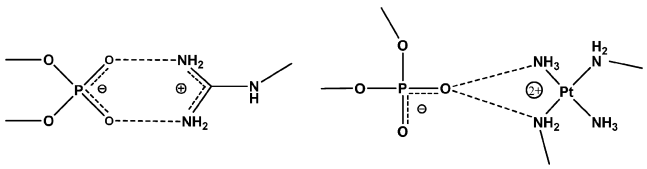

Binding modes compared to other DNA-binding ligands

Because there is some analogy between the polynuclear platinum structure (especially non-covalent compounds such as **1** and **2**) and polyamines such as spermine and spermidine, it is of interest to note that polyamines generally bind preferentially in the major groove rather than to phosphates (36). Key features in differences in recognition patterns between the two classes are the distances between amino groups and the fact that the *cis*-[Pt(NH_3)(NH_2R)] unit in fact is sterically rigid because of the strict adherence to square-planar geometry (~90° bond N-Pt-N bond angle) for Pt complexes. Polyamines are conformationally flexible and optimal distances to achieve phosphate clamp binding—provided by the square planar geometry and also to a lesser extent the sterically rigid guanidine group—are not as readily available.

Non-covalent ligand–DNA complexes are stabilized by a composite of hydrogen-bonding, van der Waals and electrostatic interactions. These interactions most generally occur within the minor groove or between base pairs (37,38). More recently Arya and coworkers have developed major groove binders (39). Appropriate

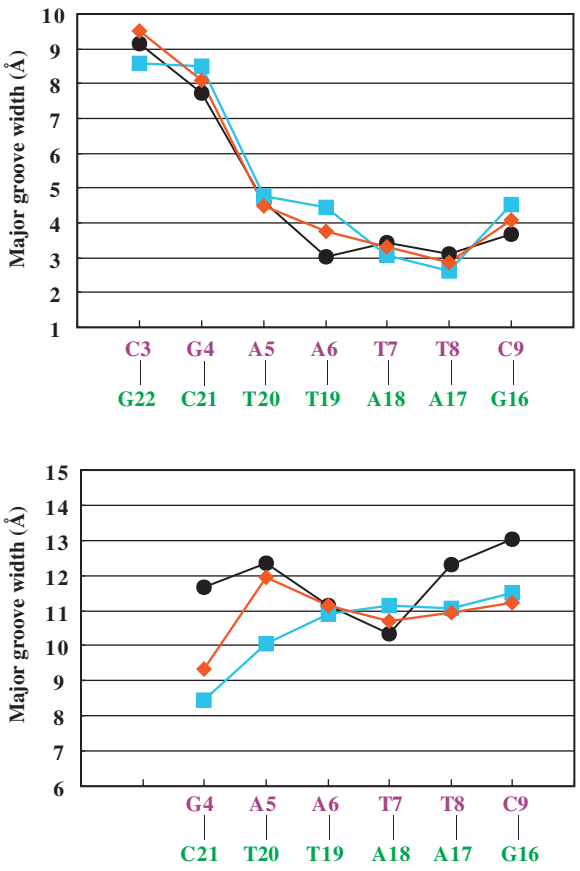

Figure 6. Minor- and major-groove widths for the DDD/TriplatinNC-A (**1**, orange diamonds), for the DDD–TriplatinNC complex (**2**, cyan squares), and for the control DDD (BDL084, black circles).

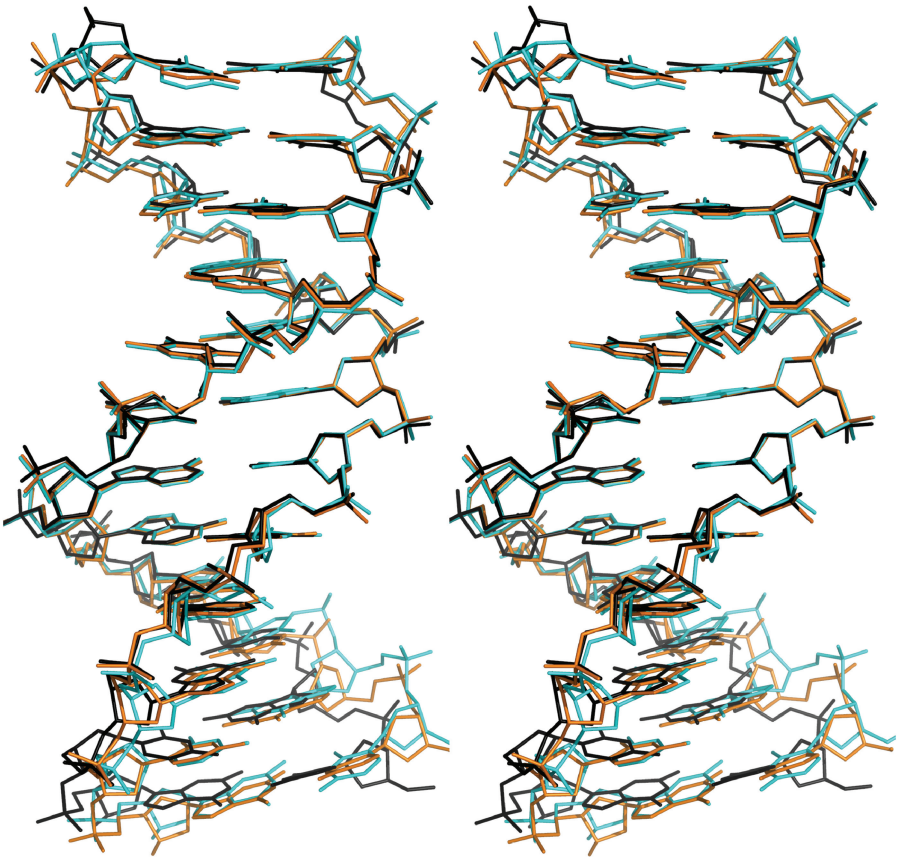

Figure 7. Superimposition of the TriplatinNC-A (1, orange) and TriplatinNC complexes (2DYW, 2, cyan) onto the control DDD (BDL084, black). Superimposition was performed based on the set of three continuous base pairs, A(6)–T(19), A(7)–T(18) and T(8)–A(17), that give the least RMS deviation of atomic positions.

combinations of modular binding elements gives high affinity and specificity (37) but, comparing all cases, the discrete nature of the Phosphate Clamp is clear.

DNA distortion

We previously suggested that a change in DNA conformation may arise upon substitution of a hydrated Mg^{2+} in the native DDD for a partially dehydrated Na^+ ion in the DDD–TriplatinNC complex (19). The Na^+ ion is located directly on the floor of the major groove (interacting with O6 of a G). It was difficult to isolate the ligand, a hydrated cation or TriplatinNC, both directly interacting with DNA, as the primary contributor to DNA deformation. In the DDD-**1** crystal structure, no hydrated cation is observed in the position of the hydrated Mg^{2+} or Na^+ in the control DDD or DDD–TriplatinNC. Accordingly, all the hydrated cations found in the control DDD, DDD–TriplatinNC, and DDD-**1** are different in atom species, hydrogen bonding properties, and interacting areas but deformation directions of TriplatinNC and **1** from the control DDD appear to be the same. Therefore, the ligands controlling the DNA deformation seem to be the trinuclear Pt(II) complexes, and hydrated cations are selected and fit to a preformed pocket of the DNA.

The work here expands the description of platinum–DNA-binding modes, and indeed metal complex–DNA interactions in general. The NDB database shows only a very limited number of crystal structures of duplex DNA bound with *cis*-platin [ntrastrand GG and the cisplatin–DNA duplex associated with the HMG protein (40), interstrand (GC)2] (41); oxaliplatin (intrastrand GG) (42) and *cis*-[$Pt(NH_3)$(cyclohexylamine)Cl_2] (intrastrand GG) (43) and a Z-DNA-forming sequence d(CGT ^{NH2}ACG)$_2$ stabilized by $[Pt(NH_3)_3]^+$ (44). With the exception of the latter, all of the DNA–platinum structures belong to the *cis*-[PtX_2(amine)$_2$] family and the work has delineated the 3D structural distortions of bifunctional binding and the factors affecting protein (HMG) recognition of the 1,2-GG intrastrand adduct. Indeed few crystal structures of non-covalently binding transition metal complexes are available—most recently the structures of a three-way DNA junction (3WJ) stabilized by metal-based supramolecular helicates have been described (45,46). The other high-resolution crystal structure entries appear limited to a sequence-specific rhodium intercalator (47,48) and the use of $[Co(NH_3)_6]^{3+}$ and $[Ru(NH_3)_6]^{3+}$ in stabilizing Z-DNA sequences (49,50).

Biological relevance of non-covalent Pt–DNA interactions

Both trinuclear compounds **1** and **2** bind to DNA exclusively by non-covalent interactions. Biophysical studies showed that the complexes stabilized duplex DNA and

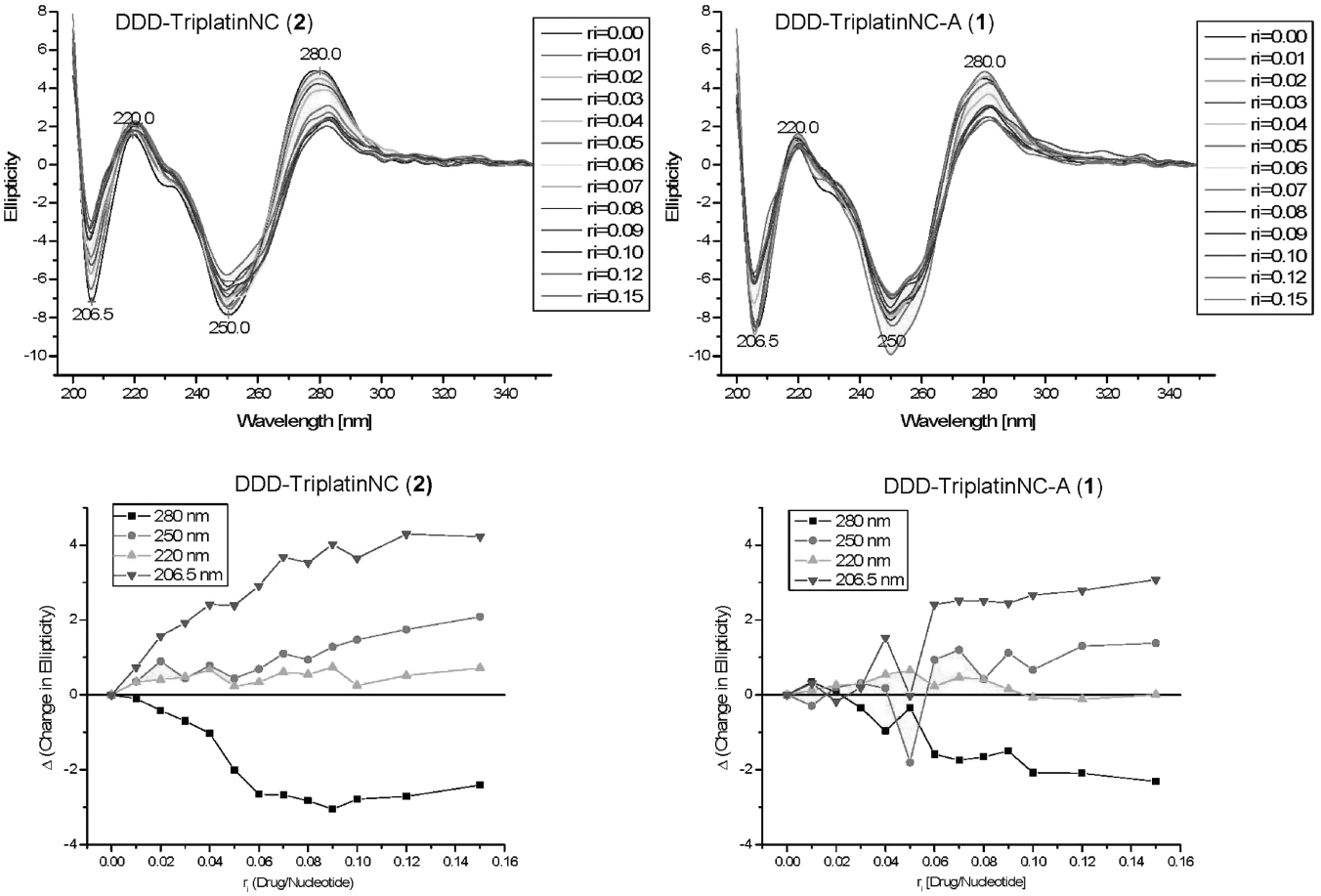

Figure 8. Circular Dichroism Spectra of DDD duplex titrated with aliquots of TriplatinNC-A (**1**) and TriplatinNC (**2**). Bottom panels show changes in ellipticity upon titration.

the higher the electrical charge of the complexes the greater the stabilization observed. The complexes induced both B → A and B → Z conformational changes in canonical DNA sequences (20). The binding affinity is sufficiently high such that they are not readily displaced from the helix by intercalators such as ethidium bromide, resulting in an essential irreversibility of the conformational change. The interaction with DNA of the minor-groove binding dye Hoechst 33 258 is cooperatively enhanced in the presence of the charged compound (22). Given the overall similarity of the binding modes, it is not surprising that the affinity of both molecules for DNA is also very similar—as would be expected since the overall binding differs only in charge and extra hydrogen bonding capability of the 'dangling' amines. Yet, the complexes differ in their biological consequences. Especially TriplatinNC (**2**, Figure 1) is cytotoxic at micromolar concentrations and exhibits *in vivo* anti-tumour activity. In contrast, **1** is ~5–10 times less potent than TriplatinNC. The enhanced cytotoxicity has been attributed to greater cellular accumulation of the 8+ species. The differences in cytotoxicity between **1** and **2** may reflect differences in cellular accumulation—the higher positive charge produces greater accumulation which may provide a stronger driving force for access to DNA, resulting in a higher frequency of phosphate clamps. Note that TriplatinNC is also significantly more potent than other non-covalent platinum compounds reported (20–23,51,52).

CONCLUSIONS

The Phosphate Clamp is a general feature of DNA complexes of PtN_4 containing non-reactive polynuclear platinum agents. The backbone selective binding is distinct from 'classic' minor-groove binding and intercalation or the more recently described major groove binding. The molecules described here contain numerous PtN4 groups acting as DNA-binding ligands and connected by flexible linkers—polymorphism in solution may arise from the number of PtN4 per binding ligand and flexible connections between them. Both minor-groove binders and intercalators have undergone extensive study for their cytotoxic and anti-tumor properties. The modular nature of the polynuclear platinum binding allows for significant further complex design (aliphatic/aromatic linkers, shorter/longer chain length, or *cis*/*trans* geometry) to enhance biological activity. Platinum-DNA binding triggers downstream cell cycle signals eventually leading to apoptosis and cell killing. Given that so little of

cisplatin actually gets to DNA, the Phosphate Clamp motif may be a much more effective method to trigger a cellular response. The absence of covalent binding to biomolecules in general may also result in less potential side effects than currently used agents. These considerations suggest that polynuclear platinum agents capable of non-covalent interactions represent a further class of platinum-based anti-tumour agents, discrete from covalently-binding mononuclear (*cis*-platin) and polynuclear (BBR3464) agents. Their overall profile relative to DNA-modifying agents deserves further investigation.

SUPPLEMENTARY DATA

Supplementary Data are available at NAR Online.

FUNDING

National Institutes of Health (RO1CA78754 to N.P.F.); the Japan Society for the Promotion of Science (to S.K., M.C. and A.O.). Funding for Open Access Charge: National Institutes of Health (grant number RO1CA78754).

Conflict of interest statement. None declared.

REFERENCES

1. Rosenberg,B., Vancamp,L., Trosko,J.E. and Mansour,V.H. (1969) Platinum compounds - a new class of potent antitumour agents. *Nature*, **222**, 385–386.
2. Rosenberg,B., Vancamp,L. and Krigas,T. (1965) Inhibition of cell division in escherichia coli by electrolysis products from a platinum electrode. *Nature*, **205**, 698–699.
3. Jamieson,E.R. and Lippard,S.J. (1999) Structure, recognition, and processing of cisplatin-DNA adducts. *Chemical Rev.*, **99**, 2467–2498.
4. Takahara,P.M., Rosenzweig,A.C., Frederick,C.A. and Lippard,S.J. (1995) Crystal structure of double-stranded DNA containing the major adduct of the anticancer drug cisplatin. *Nature*, **377**, 649–652.
5. Kelland,L.R. and Farrell,N. (2000) Platinum-based drugs in cancer therapy. In Teicher,B.A. (ed.), *Cancer Drug Discovery and Development*. Humana Press.
6. Kelland,L. (2007) The resurgence of platinum-based cancer chemotherapy. *Nature Rev. Cancer*, **7**, 573–584.
7. Farrell,N. (1993) Nonclassical platinum antitumor agents – perspectives for design and development of new drugs complementary to cisplatin. *Cancer Invest*, **11**, 578–589.
8. Hegmans,A., Berners-Price,S.J., Davies,M.S., Thomas,D.S., Humphreys,A.S. and Farrell,N. (2004) Long range 1,4 and 1,6-interstrand cross-links formed by a trinuclear platinum complex. Minor groove preassociation affects kinetics and mechanism of cross-link formation as well as adduct structure. *J Am Chem Soc*, **126**, 2166–2180.
9. Farrell,N., Qu,Y., Feng,L. and Vanhouten,B. (1990) Comparison of chemical-reactivity, cytotoxicity, interstrand cross-linking and DNA-sequence specificity of bis(platinum) complexes containing monodentate or bidentate coordination spheres with their monomeric analogs. *Biochemistry*, **29**, 9522–9531.
10. Zehnulova,J., Kasparkova,J., Farrell,N. and Brabec,V. (2001) Conformation, recognition by HMG-domain proteins and nucleotide excision repair of DNA intrastrand cross-links of novel antitumor trinuclear platinum complex BBR3464. *J. Biol. Chem.*, **276**, 22191–22199.
11. Cox,J.W., Berners-Price,S., Davies,M.S., Qu,Y. and Farrell,N. (2001) Kinetic analysis of the stepwise formation of a long-range DNA interstrand cross-link by a dinuclear platinum antitumor complex: evidence for aquated intermediates and formation of both kinetically and thermodynamically controlled conformers. *J. Am. Chem. Soc.*, **123**, 1316–1326.
12. Qu,Y., Scarsdale,N.J., Tran,M.C. and Farrell,N.P. (2003) Cooperative effects in long-range 1,4 DNA-DNA interstrand cross-links formed by polynuclear platinum complexes: an unexpected syn orientation of adenine bases outside the binding sites. *J. Biol. Inorg. Chem.*, **8**, 19–28.
13. Farrell,N. (2004) Polynuclear platinum drugs. *Metal Ions Biol. Sys.*, **41**, 252–296.
14. Kasparkova,J., Zehnulova,J., Farrell,N.P. and Brabec,V. (2002) DNA interstrand crosslinks of novel antitumor trinuclear platinum complex BBR3464. Conformation, recognition by HMG-domain proteins and nucleotide excision repair. *J. Biol. Chem.*, **277**, 48076–48086.
15. Martin,L.P., Hamilton,T.C. and Schilder,R.J. (2008) Platinum resistance: the role of DNA repair pathways. *Clin. Cancer Res.*, **14**, 1291–1295.
16. Stewart,D.J. (2007) Mechanisms of resistance to cisplatin and carboplatin. *Crit. Rev. Oncol. Hematol.*, **63**, 12–31.
17. Reed,E. (2005) ERCC1 and clinical resistance to platinum-based therapy. *Clin. Cancer Res.*, **11**, 6100–6105.
18. Manzotti,C., Pratesi,G., Menta,E., Di Domenico,R., Cavalletti,E., Fiebig,H.H., Kelland,L.R., Farrell,N., Polizzi,D., Supino,R. *et al.* (2000) BBR 3464: a novel triplatinum complex, exhibiting a preclinical profile of antitumor efficacy different from cisplatin. *Clin. Cancer Res.*, **6**, 2626–2634.
19. Komeda,S., Moulaei,T., Woods,K.K., Chikuma,M., Farrell,N.P. and Williams,L.D. (2006) A third mode of DNA binding: phosphate clamps by a polynuclear platinum complex. *J. Am. Chem. Soc.*, **128**, 16092–16103.
20. Qu,Y., Harris,A., Hegmans,A., Petz,A., Kabolizadeh,P., Penazova,H. and Farrell,N. (2004) Synthesis and DNA conformational changes of non-covalent polynuclear platinum complexes. *J. Inorg. Biochem.*, **98**, 1591–1598.
21. Harris,A.L., Yang,X., Hegmans,A., Povirk,L., Ryan,J.J., Kelland,L. and Farrell,N.P. (2005) Synthesis, characterization, and cytotoxicity of a novel highly charged trinuclear platinum compound. Enhancement of cellular uptake with charge. *Inorg. Chem.*, **44**, 9598–9600.
22. Harris,A., Qu,Y. and Farrell,N.P. (2005) Unique cooperative binding interaction observed between a minor groove binding Pt anti-tumor agent and Hoeschst dye 33258. *Inorg. Chem.*, **44**, 1196–1198.
23. Harris,A.L., Ryan,J.J. and Farrell,N.P. (2006) Biological consequences of trinuclear platinum complexes: comparison of BBR 3464 to its non-covalent Congeners. *Mol. Pharmacol.*, **69**, 666–672.
24. Wing,R., Drew,H., Takano,T., Broka,C., Takana,S., Itakura,K. and Dickerson,R.E. (1980) Crystal structure analysis of a complete turn of B-DNA. *Nature*, **287**, 755–758.
25. Shui,X., McFail-Isom,L., Hu,G.G. and Williams,L.D. (1998) The B-DNA dodecamer at high resolution reveals a spine of water on sodium. *Biochemistry*, **37**, 8341–8355.
26. Brunger,A.T., Adams,P.D., Clore,G.M., DeLano,W.L., Gros,P., Grosse-Kunstleve,R.W., Jiang,J.S., Kuszewski,J., Nilges,M., Pannu,N.S. *et al.* (1998) Crystallography & NMR system: a new software suite for macromolecular structure determination. *Acta Crystallogr. Sect. D-Biol. Crystallogr.*, **54**, 905–921.
27. Sheldrick,G.M. (1997) SHELX-97. *SHELX-97, Gottingen University, Germany*.
28. Stofer,E. and Lavery,R. (1994) Measuring the geometry of DNA grooves. *Biopolymers*, **34**, 337–346.
29. Sines,C.C., McFail-Isom,L., Howerton,S.B., VanDerveer,D. and Williams,L.D. (2000) Cations mediate B-DNA conformational heterogeneity. *J. Am. Chem. Soc.*, **122**, 11048–11056.
30. Minasov,G., Tereshko,V. and Egli,M. (1999) Atomic-resolution crystal structures of B-DNA reveal specific influences of divalent metal ions on conformation and packing. *J. Mol. Biol.*, **291**, 83–99.
31. Privé,G.G., Heinemann,U., Chandrasegaran,S., Kan,L.S., Kopka,M.L. and Dickerson,R.E. (1987) Helix geometry,

hydration, and G-A mismatch in a B-DNA decamer. *Science*, **238**, 498–504.
32. Hartmann,B., Piazzola,D. and Lavery,R. (1993) BI-BII transitions in B-DNA. *Nucleic Acids Res.*, **21**, 561–568.
33. Calnan,B.J., Tidor,B., Biancalana,S., Hudson,D. and Frankel,A. (1991) Arginine-mediated RNA recognition: the arginine fork. *Science*, **252**, 1167–1171.
34. Ban,N., Nissen,P., Hansen,J., Moore,P.B. and Steitz,T.A. (2000) The complete atomic structure of the large ribosomal subunit at 2.4 A resolution. *Science*, **289**, 905–920.
35. Klein,D.J., Schmeing,T.M., Moore,P.B. and Steitz,T.A. (2001) The kink-turn: a new RNA secondary structure motif. *EMBO J.*, **20**, 4214–4221.
36. Woods,K.K., Maehigashi,T., Howerton,S.B., Sines,C.C., Tannenbaum,S. and Williams,L.D. (2004) High-resolution structure of an extended A-tract: $[d(CGCAAATTTGCG)]_2$. *J. Am. Chem. Soc.*, **126**, 15330–15331.
37. Strekowski,L. and Wilson,B. (2007) Noncovalent interactions with DNA: an overview. *Mutat. Res.*, **623**, 3–13.
38. Geierstanger,B.H. and Wemmer,D.E. (1995) Complexes of the minor groove of DNA. *Annu. Rev. Biophys. Biomol. Struct.*, **24**, 463–493.
39. Willis,B. and Arya,D.P. (2009) Triple recognition of B-DNA. *Bioorg. Med. Chem. Lett.*, **19**, 4974–4979.
40. Takahara,P.M., Rosenzweig,A.C., Frederick,C.A. and Lippard,S.J. (1995) Crystal structure of double-stranded DNA containing the major adduct of the anticancer drug cisplatin. *Nature*, **377**, 649–652.
41. Coste,F., Malinge,J.M., Serre,L., Shepard,W., Roth,M., Leng,M. and Zelwer,C. (1999) Crystal structure of a double-stranded DNA containing a cisplatin interstrand cross-link at 1.63 Å resolution: hydration at the platinated site. *Nucleic Acids Res.*, **27**, 1837–1846.
42. Spingler,B., Whittington,D.A. and Lippard,S.J. (2001) Crystal structure of an oxaliplatin 1,2-d(GpG) intrastrand cross-link in a DNA dodecamer duplex. *Inorg. Chem.*, **40**, 5596–5602.
43. Silverman,A.P., Bu,W., Cohen,S.M. and Lippard,S.J. (2002) 2.4-Å crystal structure of the asymmetric platinum complex $[t(ammine)(cyclohexylamine)]^{2+}$ bound to a dodecamer DNA duplex. *J. Biol. Chem.*, **277**, 49743–49749.
44. Parkinson,G.N., Arvanitis,G.M., Lessinger,L., Ginell,S.L., Jones,R., Gaffney,B. and Berman,H.M. (1995) Crystal and molecular structure of a new Z-DNA crystal form: d[CGT(2-NH2-A)CG] and its platinated derivative. *Biochemistry*, **34**, 15487–15495.
45. Oleksi,A., Blanco,A.G., Boer,R., Uson,I., Aymami,J., Rodger,A., Hannon,M.J. and Coll,M. (2006) Molecular recognition of a three-way DNA junction by a metallosupramolecular helicate. *Angew Chemie, Int. Edit.*, **45**, 1227–1231.
46. Boer,D.R., Kerckhoffs,J.M., Parajo,Y., Pascu,M., Usón,I., Lincoln,P., Hannon,M.J. and Coll,M. (2010) Self-assembly of functionalizable two-component 3D DNA arrays through the induced formation of DNA three-way-junction branch points by supramolecular cylinders. *Angew. Chemie, Int. Edit.*, **49**, 2336–2339.
47. Kielkopf,C.L., Erkkila,K.E., Hudson,B.P., Barton,J.K. and Rees,D.C. (2000) Structure of a photoactive rhodium complex intercalated into DNA. *Nat. Struct. Biol.*, **7**, 117–121.
48. Pierre,V.C., Kaiser,J.T. and Barton,J.K. (2007) Insights into finding a mismatch through the structure of a mispaired DNA bound by a rhodium intercalator. *Proc. Natl Acad. Sci., USA*, **104**, 429–434.
49. Thiyagarajan,S., Rajan,S.S. and Gautham,N. (2004) Cobalt hexammine induced tautomeric shift in Z-DNA: the structure of d(CGCGCA)*d(TGCGCG) in two crystal forms. *Nucleic Acids Res.*, **32**, 5945–5953.
50. Ho,P.S., Frederick,C.A., Saal,D., Wang,A.H. and Rich,A. (1987) The interactions of ruthenium hexaammine with Z-DNA: crystal structure of a $Ru(NH_3)_6^{+3}$ salt of d(CGCGCG) at 1.2 A resolution. *J. Biomol. Struct. Dyn.*, **4**, 521–534.
51. Collins,J.G. and Wheate,N.J. (2004) Potential adenine and minor groove binding platinum complexes. *J. Inorg. Biochem.*, **98**, 1578–1584.
52. Wheate,N.J., Cutts,S.M., Phillips,D.R., Aldrich-Wright,J.R. and Collins,J.G. (2001) The binding of $[(en)Pt(\mu\text{-}dpzm)_2Pt(en)]^{4+}$ to G/C-rich regions of DNA. *J. Inorg. Biochem.*, **84**, 119–127.